Behaviors of sodium and calcium ions at the borosilicate glass–water interface: Gaining new insights through an ab initio molecular dynamics study

Hicham Jabraoui, Thibault Charpentier, Stephane Gin, Jean-Marc Delaye, Rodolphe Pollet

Behaviors of sodium and calcium ions at the borosilicate glass−water interface: gaining new insights through an *ab initio* molecular dynamics study

Hicham Jabraoui,[1, a)] Thibault Charpentier,[1] Stéphane Gin,[2] Jean-Marc Delaye,[2] and Rodolphe Pollet[1]
[1)] *Université Paris-Saclay, CEA, CNRS, NIMBE, F-91191 Gif-sur-Yvette cedex, France*
[2)] *CEA, DES, ISEC, DE2D, University of Montpellier, Marcoule, F−30207 Bagnols−sur−Ceze, France*

(Dated: 5 March 2022)

We study reactivity and leaching at the calcium sodium borosilicate (CNBS)−water interface by means of a Car−Parrinello *ab initio* molecular dynamics (AIMD) simulation over a simulation time of 100 ps. With an emphasis on the comparison between the behavior of Ca^{2+} and Na^{+} cations at the CNBS glass-water interface, different mechanism events during the trajectory are revealed, discussed and correlated with other density functional theory calculations. We show that Na^{+} ions can be released in solution while Ca^{2+} cannot leave the surface of CNBS glass. This release is correlated with the vacancy energy of Ca^{2+} and Na^{+} cations. Here we found that the CNBS structure with the Na^{+} cation vacancy is energetically more favorable than the structure with the Ca^{2+} cation vacancy. The calcium adsorption site has been shown to have a greater affinity for water than can be found in the case of the sodium site, demonstrating that affinity may not be considered a factor major controlling the release of cations from the glass to the solution.

I. Introduction

Borosilicate glass has proven to be a good material for the safe long−term storage of radioactive waste[1–4]. It is envisioned that these nuclear glasses will be subject to permanent deep geological storage with low permeability and a stable environment[5]. However, after a long period of up to thousands of years, the diffusing groundwater can slowly reach the glass, which will cause a significant change in the chemical and physical properties of glass[6–8]. It is therefore necessary to understand the mechanisms at the origin of the corrosion of these glasses by the aqueous solution in order to assess their environmental impact and the safety of the geological repository[5]. Having a thorough understanding of the glass−water interface also serves to control many other glass applications−based borosilicate material such as photo multiplier tubes, display technology, biomedical devices, windows in architectures,etc[9–12].

In our recent Car−Parrinello *ab initio* molecular dynamics (CP-AIMD) simulations of the sodium borosilicate (NBS) glass−water interface with an emphasis on the behaviors of B^{III} and B^{IV}[13] sites, we found that the high affinity between sodium and water dominates the NBS glass interface, which leads to such events: i) the release of sodium in liquid water, ii) dissociation of the water molecules on the boron atom with 3−coordination since these are the most exposed units on the surface of the glass which lead both to the formation of boronol and silanol groups. In another study, the ionic exchange (Na^{+} and H_3O^{+}) in a borosilicate glass was investigated with a static DFT calculation[14], and the authors suggested that an ionic exchange initiates a depolymerization of the glass network. In another DFT study coupled with NEB calculations, Zapol *et al*[15] estimated the reaction barriers for hydrolysis reactions on the surface of borosilicate glass and suggested that under neutral, basic and acidic conditions, the reaction barrier either of B —— O —— B or of B —— O —— Si is lower than Si —— O —— Si, while the reaction barriers under acidic conditions for the dissolution of B —— O —— B and B —— O —— Si bridges are considerably reduced compared to neutral and basic conditions. From Monte Carlo simulations, it has been shown that as the weathering progresses, a stationary state is reached, in which a protective layer enriched in silicon atoms forms between the pristine glass and the solution after release of soluble elements (boron, Na^{+})[16–19]. From these previous investigations, we can estimate that the glass−water interface NBS showed the release of B, Si and Na^{+}.

Here we are looking at a more realistic simplified model of nuclear borosilicate glass that contains calcium oxide and sodium oxide, in which the current glass is depicted under the chemical composition as follows $10(CaO)15(Na_2O)24(B_2O_3)51(SiO_2)$, denoted by CNBS in the rest of text. In the present work, we have used Born−Oppenheimer MD (BOMD) simulations to simulate CNBS glass in which we can get a good description of borate-based glass with the presence of boroxol rings[20] and good distribution of Na^{+} and Ca^{2+} cations in the borosilicate glass matrix[21]. To simulate the CNBS−glass interface we performed an AIMD simulation during which we can assess the events that may appear when the CNBS glass interacts with water at a certain temperature. AIMD simulations proved to be a reliable tool for predicting a glassy state of a borosilicate−based glassy material[20,22]. CP-AIMD simulations have been widely proven to provide reliable results to elucidate water−mineral interface[23–27] and specially water−glass interface[13,28,29]. Static DFT calculations were also used to provide some insights in terms of affinity between the water molecule and cation−based adsorption sites as well as the possibility of cationic vacancy formation. DFT calculations have shown great success in studying the behavior of a water molecule with cationic sites in various silica materials[30–37].

[a)] Electronic mail: hicham.jabraoui@cnrs.fr

Our current attempt is to provide the effect of calcium on the event shown above at the glass−water interface as well as to compare the behavior of calcium and sodium with respect to water molecules. Noteworthy, the investigation of the CNBS glass−water interface at atomic scale is, to our knowledge, the first studied.

This article is arranged as follows: the second section provides details on the computational methodology to simulate the studied borosilicate glass and the glass-water interface, the third section presents and discusses the relevant results of the glass CNBS−water interface. Finally, we present the main conclusions.

II. Computational details

A. AIMD simulation for CNBS glass modeling

We used the CP2K package[38] to perform BOMD simulations in order to model the glassy state of CNBS glass. MD simulations based on DFT are known to reproduce experimental results more accurately than those based on force fields where our subject is to have a good Na/Ca mixing interaction in bulk and surface structures[39]. Here, the GGA−PBE functional[40] was used, including D3 dispersion corrections[41] to account for the long range van der Waals interactions. TZVP Gaussian Basis sets[42] combined to GTH potentials[43] (as provided by the CP2K packages) were used for all atomic species, with an energy cutoff of 41.16 Ry. The BOMD simulations were performed using a standard melt−quench procedure of the initial structure generated by a classic MD simulation as described in SI with a composition of 10(CaO)15(Na_2O)24(B_2O_3)51(SiO_2) and a density of 2.53 g/cm^3: i) The system was first heated up to 2500 K with a NVT run of 15 ps followed by a NVE run during 10 ps to equilibrate the system in the liquid state; ii) quench to 300 K during 10 ps iii) NPT run at 300 K to equilibrate to system at the glass density (5 ps); iv) final NVE run at 300 K to further equilibrate the structure at the mean density determined from the last ps of the NPT run. The MD timestep was chosen to 0.5 fs to ensure good energy conservation. The initial classical MD structure is generated using the same force fields and following the same melt−quench procedure as used in our previous study[13]. The structural details of our CNBS glass obtained by BOMD simulation are shown in Table S1.

B. Modeling of the glass– water interface

CPMD software package[44] is used to perform Car−Parrinello *ab initio* MD simulations[45] of the water−glass interface. CP-AIMD was chosen here for a comparison with previous simulations of the NBS glass−water interface[13]. For building the structural model of the CNBS glass−water interface, we first create the CNBS glass surface using the cleaving process in which the CNBS bulk glass simulation box is stretched in a Z direction, creating a vacuum above the glass surface. The cleaved CNBS glass surface was annealed at 363 K for 10 ps in the NVT ensemble using the CP-AIMD simulation, which is called in the rest of the paper by non−hydrated CNBS surface. The simulated surface was then concatenated with a water film containing 85 water molecules to build the initial water−CNBS interface model. This interface fills an orthorhombic cell of 17.67×15.83×24.98 Å^3 (Figure 1). This model was subjected to the annealing process at 363 K over 100 ps in the NVT ensemble using CP-AIMD simulation to obtain the governing event at the CNBS glass-water interface.

To run our surface and interface simulation CP-AIMD, PBE+D2 level of theory[46], plane wave basis set and Vanderbilt pseudopotentials[47] with an energy cutoff of 30 Ry were used. Please note that the $2s2p$ semicore electrons are not included in the valence space for sodium (one valence electrons) whereas the calcium pseudopotential includes the $3s3p$ semicore electrons (ten valence electrons), both pseudopotentials including nonlinear core corrections. The time step used for all CP-AIMD simulations was 4.8 a.u. (about 0.116 fs) and a fictitious electronic mass of 700 a.u, while the kinetic energy of ions and electrons was controlled by Nosé−Hoover chain thermostats. It should be noted that the hydrogen atoms have been replaced by deuterium atoms to preserve adiabaticity in the CP-AIMD simulations. Scheme 1 clearly shows the stages of our methodologies for simulating the glass-water−CNBS interface. After shedding light on the CP-AIMD trajectory events, static DFT calculations using VASP packages (see SI details) were run to quantify single-water molecule adsorption at CNBS glass surface sites with emphasis on those based on Na^+ or Ca^{2+} cations and to calculate the vacancy formation energy of Na^+ and Ca^{2+} cations.

III. Results and Discussion

A. Interface characterisation

In the present study, we first simulated CNBS glass using BOMD simulations providing a good description of the structure of the borate−based glass with the presence of boroxol rings[20] (see Figure S1) and a good distribution of Na^+ and Ca^{2+} cations in the borosilicate glass matrix[21]. Subsequently, the CNBS glass is cleaved in the Z direction and assembled with a water film to simulate the CNBS glass−water interface using a CP-AIMD simulation over 100 ps at 363 K (see Scheme 1). Our attempt here is to give a good observation of the CNBS glass− water interface by emphasizing the comparison between the behaviors of sodium and calcium. In this section, we characterize the environment of the different chemical species composing our interface over the whole simulation time.

The radial distribution function (RDF) and its accumulated function can provide the average characterization of the glass−water interface over a simulation time in terms of the average distance between the different species and the different components of the glass and the average coordination number. Figure 2(a−b) summarizes the impact of water on former (Si and B) and modifier/compensator of charge components (Na and Ca) where we give in pairs the distances between these species and the oxygen of water molecules and the number of molecules of water involved in the evolution of the latter species. For Na — O_W, the first peak is at 2.33 Å, while the position of the secondary peak with a lower intensity is located around 4.39 Å. For Ca — O_W, the first peak and the lower second intensity peaks are located at 2.40 Å and 4.30 Å, respectively. These results are in good

agreement with our previous AIMD for the glass-water interface NBS[13]. The second peak that appeared with the two cations means that the influence of both Ca^{2+}ions and Na^{+} ions is sufficiently extended in the deep layers of the water. This suggests that the first solvation shell of $Ca^{2+}$and Na^{+} binds to the second shell via H−bonds of a distance about 2 Å. This is in agreement with previous AIMD simulations of the quartz−water interface in which ions have been shown to rearrange H_2O molecules[48]. Noteworthy, Na —— O_W and Ca —— O_W distances are close to typical Na−O distances found in the bulk glass (see Table 1 SI). This behavior is more pronounced in Na —— O than Ca —— O (see Table I), which means that water can shift Na^{+} ions easier than Ca^{2+}. However, when the water molecules are brought into contact with the CNBS surface glass, the water contribute to reform Na and Ca polyhedra by 1.01 and 0.35 of O_W, respectively(see Figure 2(c−d)) where ACN of Ca increases from 6.522 (non−hydrated surface) to 6.871 while ACN of Na increases from 5.306 (non−hydrated surface) to 6.314 (hydrated surface) (see Table I). This suggests that the water is reforming the vitreous region around Na slightly more than around Ca. Compared to other glass−water interfaces, Tilocca *et al*[28] studied the water−bioactive glass interface using AIMD and they found that main interactions involving water molecules at the interface, in addition to the H−bonds between them, are with Na^{+} and Ca^{2+} cations, with Na —— O_W and Ca —— O_W distances of about 2.34 and 2.45 Å, respectively, which are close to that presented in their glass bulk[49,50].
For the glass former elements Si —— O_W and B —— O_W, the first peaks are at 1.655 Å and 1.375 Å, respectively. It is also shown a shoulder with low intensity at 1.365 Å before having a fine peak of B —— O_W which is attributed to reforming of B^{III} units with an insignificant amount at the surface where the fine peak is attributed to reforming of B^{IV} units at the surface of the glass. By comparing the effect of water on Si and on B, we found that as the water being in contact with the CNBS surface glass, B —— O bonds length take values close to what can be found in the CNBS bulk. However, the Si —— O bond is independent of the presence of water where we have the same distance in both the non−hydrated and hydrated surface as in the original bulk before the cleavage process.

For $g_{H-O_G}(r)$, the first peak is at 1.00 Å representing the formation of isolated silanol groups (SiO_GH) and boronol groups (B —— O_GH) and one germinal silanol group (see Figure 3a). The appearance of germinal groups with insignificant amounts compared to other types of oxygen−bearing functional groups is also shown in the long simulation trajectory by the ReaxFF MD simulation of the sodium aluminosilicate glass−water interface[51]. A second peak located at 1.64 Å assigned for H−bonds. The formation of isolated silanol and boronol groups serves as a signature both for the occupation of the defect formed (Si^{III}) after the cleavage process and for the depolymerization of the structure by breaking the Si —— O —— Si and Si —— O —— B after dissociation of water molecules. This observation is in good agreement with previous ICP−AES (induced coupled plasma–atomic emission spectroscopy) studies and MC simulations[52] for boronol group formations and NMR studies for silanol group formations[53,54]. The formation of silanol and boronol groups from the proton or O_WH proceed in two stages; the first stage is an increase during the first 10 ps reaching 9 silanol groups and 6 boronol groups while the second stage is a plateau evolution where the number of silanols fluctuates around 9 silanol groups and 6 boronol groups (see Figure 3b). The first stage is mainly correlated with the occupation of defects on the CNBS glass surface (due to the cleavage process) by H^{+} and OH^{-} resulting from water dissociations while the fluctuation at the second stage is correlated with structural Grotthuss diffusion between silanol groups and water molecules[13,55]. Figure 3(c−e) shows germinal oxygen−bearing functional group, boronol and silanol groups where two last groups are dominant. These functional groups enhance the affinity between water and CNBS surface glass, which means that when the surface is stabilized by these groups, events at the glass−water interface become more pronounced. Here we found that a water molecule can be adsorbed on the hydrated surface by forming two H bonds with two silanols. This observation is in agreement with a previous *ab initio* investigation of water in a silicatlite−1[56].

B. Sodium− calcium release

In our previous study[13], we showed the higher affinity of Na^{+} ions towards water molecules compared to other species in NBS glass. In this previous investigation, we assumed that this strong affinity can be directly involved in the mechanisms of dissolution of glass, in which a sodium ion was seen to emerge from the surface thanks to its hydration and the participation of sodium atoms on the surface in the process of penetration of water molecules in the first layers of the NBS glass[13].

In our current study, we aim at comparing the behavior of sodium and calcium in borosilicate glass when in contact with water molecules. Herein, we found that a sodium ion can be release from the CNBS glass surface as shown in Figure 4. The release of sodium in liquid water takes place in three stages throughout the simulation:

- Over the first 5 ps; the Na^{+} ion adsorbs around two water molecules near the surface at a distance of 2.42 Å and vibrates around its initial position (see Figure 5a).
- From 5 ps to 50 ps; Na^{+} goes away from its initial position at a distance of about 2 Å during which the sodium is surrounded by 3−4 water molecules at an average distance of 2.38 Å (see Figure 5b).
- From 50 ps to the end of our simulation, this sodium continues to penetrate deeply into liquid water in a linear fashion up to 4.75 Å over 19 ps, then finally this hydrated Na^{+} ion slightly returns towards the surface; during this step the number of surrounding water molecules is about 4−5 H_2O molecules at a distance of 2.35 Å (see Figure 5c).

In addition to this first example, another sodium ion has similarly been released in solution (see Figure S2). In general, the released Na^{+} ion into the solution can be surrounded

TABLE I. Pairwise interatomic distances and average coordination number (ACN) of B−O, Si−O, Na−O, and Ca−O bonds in CNBS bulk glass, in the non−hydrated CNBS surface (cleaved surface without the presence of water molecules), in the hydrated surface (extract from the trajectory of the CNBS glass−water interface). For the non−hydrated surface glass and the bulk glass (before the cleavage process), RDF (short interatomic distance) and their accumulative functions (ACN) are obtained after running a NVT relaxation simulation at 363 K over 5 ps, while the values corresponding to the hydrated area (interface) were calculated over the last 50 ps of the NVT simulation at 363 K.

	Bulk		Non−hydrated surface		Hydrated surface	
Pair	d (Å)	ACN	d (Å)	ACN	d (Å)	ACN
B —— O	1.41	3.36	1.38	3.12	1.38	3.24
Si —— O	1.66	4.04	1.66	3.91	1.66	4.00
Na —— O	2.35	6.45	2.34	5.31	2.34	6.31
Ca —— O	2.38	6.91	2.31	6.52	2.315	6.87

ACN± 0.1 & interatomic distance $r_{i^*j} \pm 0.05$.

by 4 to 6 water molecules, as shown in Figure 5 and Table II. This is in good agreement with previous AIMD simulations[13], other AIMD simulations[57–62] and experimental investigations of the hydrated Na^+ ions[62–66]. Our previous ReaxFF MD simulation of the NAS glass−water interface showed that the release of the Na^+ ion is due to the initial exchange of $Na^+ \rightleftharpoons H^+$ at the interface involving the dissociation of water close to a Na^+ —— NBO pair[51].

Regarding the behavior of Ca^{2+} ions with water at the interface, our trajectory shows no release of calcium into the solution although Na^+ and Ca^{2+} are exposed in the same way to water molecules. Figure 6 shows a representative case of the behavior of Ca with water molecules at the interface. Here it is clearly shown that calcium is not able to leave the glass surface even though it can itself attract more than 3 water molecules at a distance of about 2.42 Å. This number of surrounding water molecules is not enough to ensure the hydration of Ca. From a previous CP-AIMD simulation[67], it was shown that Ca^{2+} ions are hydrated by 6 surrounding water molecules at distances between 2.49 and 2.55 Å, respectively. From classical MD or MC simulations[68,69], the nearest neighbor and the coordination number obtained ranges between 7−9.3 and 2.39−2.54 Å, respectively. The adsorption energy of water onto the site of Ca adsorption is higher than onto the Na adsorption site by 19.39 kJ/mol (see Figure 7 and SI for more DFT calculations).

The higher affinity between Ca and water molecules compared to Na and water molecules is also demonstrated by the fact that at the interface, the majority of Ca^{2+} ions attract 3 water molecules while the majority of Na ions can only attract one water molecule (see Table II). This means that the affinity of the glass ion and water may not be a criterion for ion release into solution. However, by calculating the vacancy formation energy of Ca^{2+} and Na^+ ions using DFT (see SI calculations), we found that the CNBS glass with sodium vacancy (E_{vac}=350.24 kJ/mol) is energetically more favorable than CNBS structure with calcium vacancy E_{vac}=430.32 kJ/mol) by about 80.08 kJ/mol. Noteworthy, the vacancy energy for each cation is computed as the average of the energy of four CNBS glass configurations with one-missing cation.

TABLE II. Different coordination numbers (CN) and the average coordination number of Na and Ca at the interface with respect to oxygen of water molecules calculated over the last 45 ns. See the corresponding curves in Figure S3, Figure S4 and Figure S5, as indicated the coordination numbers were computed for a cutoff of 3Å.

CN	0	1	2	3	4	5	6	ACN
Na %	52.6	20.2	9.1	6.2	5.9	4.4	1.7	1.1
Ca %	49.9	14.4	11.7	14.5	9.5	-	-	1.2

IV. Conclusion

In the context of the degradation of nuclear waste forms, our study attempts to better understand the reactivity and leaching at the CNBS glass−water interface. This study sheds the light on a basic machanism that take place during glass alteration and that was poorly understood. By correlating the AIMD trajectory and DFT calculations, we show that the Ca^{2+} and Na^+ ions behave differently at the glass CNBS−water interface in which the Na^+ ion can be released into water while Ca^{2+} remains on the surface of CNBS glass but adsorbs more water molecules than sodium on the surface of CNBS glass. The higher affinity between calcium and water than between sodium and water is also confirmed by the fact that the gas phase water molecule adsorbs more onto calcium adsorption sites than onto sodium. The susceptibility of sodium to be released into the water can be correlated with the vacancy energy of the cation where the CNBS structure with the Na^+ cation vacancy is energetically more favorable than the structure with the Ca^{2+} cation vacancy.

Conflicts of interest

All of the authors claim that there is no competition for personal relationships or financial interests that may have influenced the publication of the study reported in this paper.

Supporting Information

Details of the DFT calculation, characterization of our CNBS glass before starting the simulation of the CNBS glass-water interface, and more in-depth analysis of this interface.

acknowledgement

Authors thank Programmes Transversaux de Compétences « Simulation Numérique » (ALTERVER) of the French Alternative Energies and Atomic Energy Commission (CEA) for financial support. This work was granted access to the HPC/AI resources of TGCC under the allocation 2021-A0100810825 made by GENCI.

Author information

Hicham Jabraoui− Université Paris-Saclay, CEA, CNRS, NIMBE, F-91191 Gif-sur-Yvette cedex, France; https://orcid.org/0000-0003-1201-8358
Email: hicham.jabraoui@cnrs.fr, hicham.jabraoui@gmail.com
Thibault Charpentier− Université Paris-Saclay, CEA, CNRS, NIMBE, F-91191 Gif-sur-Yvette cedex, France;

https://orcid.org/0000-0002-3034-1389
Stéphane Gin−CEA, DES, ISEC, DE2D, University of Montpellier, Marcoule, F−30207 Bagnols−sur−Ceze, France; https://orcid.org/0000-0002-1950-9195
Jean-Marc Delaye−CEA, DES, ISEC, DE2D, University of Montpellier, Marcoule, F−30207 Bagnols−sur−Ceze, France; https://orcid.org/0000-0002-1311-642X
Rodolphe Pollet− Université Paris-Saclay, CEA, CNRS, NIMBE, F-91191 Gif-sur-Yvette cedex, France; https://orcid.org/0000-0003-1081-3323

[1] M. I. Ojovan and W. E. Lee, "Glassy wasteforms for nuclear waste immobilization," Metallurgical and Materials Transactions A **42**, 837–851 (2011).
[2] W. J. Weber, R. C. Ewing, C. A. Angell, G. W. Arnold, A. N. Cormack, J. M. Delaye, D. L. Griscom, L. W. Hobbs, A. Navrotsky, D. L. Price, *et al.*, "Radiation effects in glasses used for immobilization of high-level waste and plutonium disposition," Journal of Materials Research **12**, 1946–1978 (1997).
[3] S. Peuget, J.-M. Delaye, and C. Jégou, "Specific outcomes of the research on the radiation stability of the french nuclear glass towards alpha decay accumulation," Journal of Nuclear Materials **444**, 76–91 (2014).
[4] S. Gin, A. Abdelouas, L. J. Criscenti, W. L. Ebert, K. Ferrand, T. Geisler, M. T. Harrison, Y. Inagaki, S. Mitsui, K. T. Mueller, *et al.*, "An international initiative on long-term behavior of high-level nuclear waste glass," Materials Today **16**, 243–248 (2013).
[5] J. D. Vienna, J. V. Ryan, S. Gin, and Y. Inagaki, "Current understanding and remaining challenges in modeling long-term degradation of borosilicate nuclear waste glasses," International Journal of Applied Glass Science **4**, 283–294 (2013).
[6] T. Geisler, A. Janssen, D. Scheiter, T. Stephan, J. Berndt, and A. Putnis, "Aqueous corrosion of borosilicate glass under acidic conditions: a new corrosion mechanism," Journal of Non-Crystalline Solids **356**, 1458–1465 (2010).
[7] S. Gin, P. Jollivet, M. Fournier, F. Angeli, P. Frugier, and T. Charpentier, "Origin and consequences of silicate glass passivation by surface layers," Nature Communications **6**, 1–8 (2015).
[8] S. Gin, P. Jollivet, G. B. Rossa, M. Tribet, S. Mougnaud, M. Collin, M. Fournier, E. Cadel, M. Cabie, and L. Dupuy, "Atom-probe tomography, tem and tof-sims study of borosilicate glass alteration rim: a multi-scale approach to investigating rate-limiting mechanisms," Geochimica et Cosmochimica Acta **202**, 57–76 (2017).
[9] L. Wondraczek, J. C. Mauro, J. Eckert, U. Kühn, J. Horbach, J. Deubener, and T. Rouxel, "Towards ultrastrong glasses," (2011).
[10] S. Collaboration *et al.*, "The sudbury neutrino observatory," in *American Institute of Physics Conference Series*, Vol. 533 (2000) pp. 118–123.
[11] J. E. Shelby, *Introduction to glass science and technology* (Royal Society of Chemistry, 2020).
[12] N. Stone-Weiss, H. Bradtmüller, H. Eckert, and A. Goel, "Composition–structure–solubility relationships in borosilicate glasses: Towards a rational design of bioactive glasses with controlled dissolution behavior," ACS Applied Materials & Interfaces , https://doi.org/10.1021/acsami.1c07519 (2021).
[13] H. Jabraoui, T. Charpentier, S. Gin, J.-M. Delaye, and R. Pollet, "Atomic insights into the events governing the borosilicate glass–water interface," The Journal of Physical Chemistry C **125**, 7919–7931 (2021).
[14] G. Geneste, F. Bouyer, and S. Gin, "Hydrogen–sodium interdiffusion in borosilicate glasses investigated from first principles," Journal of Non-Crystalline Solids **352**, 3147–3152 (2006).
[15] P. Zapol, H. He, K. D. Kwon, and L. J. Criscenti, "First-principles study of hydrolysis reaction barriers in a sodium borosilicate glass," International Journal of Applied Glass Science **4**, 395–407 (2013).
[16] C. Cailleteau, F. Angeli, F. Devreux, S. Gin, J. Jestin, P. Jollivet, and O. Spalla, "Insight into silicate-glass corrosion mechanisms," Nature Materials **7**, 978–983 (2008).
[17] S. Kerisit and E. M. Pierce, "Monte carlo simulations of the dissolution of borosilicate glasses in near-equilibrium conditions," Journal of Non-Crystalline Solids **358**, 1324–1332 (2012).
[18] A. Jan, J.-M. Delaye, S. Gin, and S. Kerisit, "Monte carlo simulation of the corrosion of irradiated simplified nuclear waste glasses," Journal of Non-Crystalline Solids **519**, 119449 (2019).
[19] S. Kerisit and J. Du, "Monte carlo simulation of borosilicate glass dissolution using molecular dynamics-generated glass structures," Journal of Non-Crystalline Solids **522**, 119601 (2019).
[20] G. Ferlat, T. Charpentier, A. P. Seitsonen, A. Takada, M. Lazzeri, L. Cormier, G. Calas, and F. Mauri, "Boroxol rings in liquid and vitreous b2o3 from first principles," Physical Review Letters **101**, 065504 (2008).
[21] S. K. Lee and J. F. Stebbins, "Nature of cation mixing and ordering in na-ca silicate glasses and melts," The Journal of Physical Chemistry B **107**, 3141–3148 (2003).
[22] T. Ohkubo, S. Urata, Y. Imamura, T. Taniguchi, N. Ishioka, M. Tanida, E. Tsuchida, L. Deng, and J. Du, "Modeling the structure and dynamics of lithium borosilicate glasses with ab initio molecular dynamics simulations," The Journal of Physical Chemistry C **125**, 8080–8089 (2021).
[23] R. Pollet, C. Clavaguéra, and J.-P. Dognon, "Ultrasoft pseudopotentials for lanthanide solvation complexes: Core or valence character of the 4 f electrons," The Journal of chemical physics **124**, 164103 (2006).
[24] W. Langel and M. Parrinello, "Hydrolysis at stepped mgo surfaces," Physical Review Letters **73**, 504 (1994).
[25] W. Langel and M. Parrinello, "Ab initio molecular dynamics of h2o adsorbed on solid mgo," The Journal of chemical physics **103**, 3240–3252 (1995).
[26] D. Marx and J. Hutter, *Ab initio molecular dynamics: basic theory and advanced methods* (Cambridge University Press, 2009).
[27] S. Khan, R. Pollet, R. Vuilleumier, J. Kowalewski, and M. Odelius, "An ab initio casscf study of zero field splitting fluctuations in the octet ground state of aqueous [gd (iii)(hpdo3a)(h2o)]," The Journal of Chemical Physics **147**, 244306 (2017).
[28] A. Tilocca and A. N. Cormack, "Modeling the water-bioglass interface by ab initio molecular dynamics simulations," ACS Applied Materials & Interfaces **1**, 1324–1333 (2009).
[29] A. Tilocca and A. N. Cormack, "The initial stages of bioglass dissolution: a car–parrinello molecular-dynamics study of the glass–water interface," Proceedings of the Royal Society A: Mathematical, Physical and Engineering Sciences **467**, 2102–2111 (2011).
[30] I. Khalil, H. Jabraoui, S. Lebègue, W. J. Kim, L.-J. Aguilera, K. Thomas, F. Maugé, and M. Badawi, "Biofuel purification: Coupling experimental and theoretical investigations for efficient separation of phenol from aromatics by zeolites," Chemical Engineering Journal **402**, 126264 (2020).
[31] H. Jabraoui, I. Khalil, S. Lebègue, and M. Badawi, "Ab initio screening of cation-exchanged zeolites for biofuel purification," Molecular Systems Design & Engineering **4**, 882–892 (2019).
[32] J. Du and J. M. Rimsza, "Atomistic computer simulations of water interactions and dissolution of inorganic glasses," npj Materials Degradation **1**, 1–12 (2017).
[33] E. P. Hessou, H. Jabraoui, I. Khalil, M.-A. Dziurla, and M. Badawi, "Ab initio screening of zeolite y formulations for efficient adsorption of thiophene in presence of benzene," Applied Surface Science , 148515 (2020).
[34] A. Pelmenschikov, J. Leszczynski, and L. G. Pettersson, "Mechanism of dissolution of neutral silica surfaces: Including effect of self-healing," The Journal of Physical Chemistry A **105**, 9528–9532 (2001).
[35] L. J. Criscenti, J. D. Kubicki, and S. L. Brantley, "Silicate glass and mineral dissolution: calculated reaction paths and activation energies for hydrolysis of a q3 si by h3o+ using ab initio methods," The Journal of Physical Chemistry A **110**, 198–206 (2006).
[36] E. Berardo, A. Pedone, P. Ugliengo, and M. Corno, "Dft modeling of 45s5 and 77s soda-lime phospho-silicate glass surfaces: clues on different bioactivity mechanism," Langmuir **29**, 5749–5759 (2013).
[37] G. Y. Gor and N. Bernstein, "Adsorption-induced surface stresses of the water/quartz interface: Ab initio molecular dynamics study," Langmuir **32**, 5259–5266 (2016).
[38] J. Hutter, M. Iannuzzi, F. Schiffmann, and J. VandeVondele, "cp2k: atomistic simulations of condensed matter systems," Wiley Interdisciplinary Reviews: Computational Molecular Science **4**, 15–25 (2014).
[39] S. Ispas, M. Benoit, P. Jund, and R. Jullien, "Structural and electronic properties of the sodium tetrasilicate glass na 2 si 4 o 9 from classical and ab initio molecular dynamics simulations," Physical Review B **64**, 214206 (2001).

[40]J. P. Perdew, K. Burke, and M. Ernzerhof, "Generalized gradient approximation made simple," Physical Review Letters **77**, 3865 (1996).
[41]S. Grimme, J. Antony, S. Ehrlich, and H. Krieg, "A consistent and accurate ab initio parametrization of density functional dispersion correction (dft-d) for the 94 elements h-pu," The Journal of chemical physics **132**, 154104 (2010).
[42]J. VandeVondele and J. Hutter, "Gaussian basis sets for accurate calculations on molecular systems in gas and condensed phases," The Journal of chemical physics **127**, 114105 (2007).
[43]S. Goedecker, M. Teter, and J. Hutter, "Separable dual-space gaussian pseudopotentials," Physical Review B **54**, 1703 (1996).
[44]D. Hutter, A. Alavi, T. Deutsch, M. Bernasconi, S. Goedecker, and M. Parrinello, "Cpmd. copyright ibm corp 1990–2019, copyright mpi für festkörperforschung stuttgart 1997–2001, 2020,".
[45]R. Car and M. Parrinello, "Unified approach for molecular dynamics and density-functional theory," Physical Review Letters **55**, 2471 (1985).
[46]F. Neese, "Wires comput. mol. sci. 2012, 2, 73; b) s. grimme," J. Comput. Chem **27**, 1787 (2006).
[47]D. Vanderbilt, "Soft self-consistent pseudopotentials in a generalized eigenvalue formalism," Phys. Rev. B **41**, 7892–7895 (1990).
[48]M. J. DelloStritto, J. D. Kubicki, and J. O. Sofo, "Effect of ions on h-bond structure and dynamics at the quartz (101)–water interface," Langmuir **32**, 11353–11365 (2016).
[49]H. Jabraoui, M. Malki, A. Hasnaoui, M. Badawi, S. Ouaskit, S. Lebègue, and Y. Vaills, "Thermodynamic and structural properties of binary calcium silicate glasses: insights from molecular dynamics," Physical Chemistry Chemical Physics **19**, 19083–19093 (2017).
[50]H. Jabraoui, Y. Vaills, A. Hasnaoui, M. Badawi, and S. Ouaskit, "Effect of sodium oxide modifier on structural and elastic properties of silicate glass," The Journal of Physical Chemistry B **120**, 13193–13205 (2016).
[51]H. Jabraoui, S. Gin, T. Charpentier, R. Pollet, and J.-M. Delaye, "Leaching and reactivity at the sodium aluminosilicate glass−water interface: Insights from a reaxff molecular dynamics study," The Journal of Physical Chemistry C (2021), DOI: 10.1021/acs.jpcc.1c07266.
[52]C. Cailleteau, C. Weigel, A. Ledieu, P. Barboux, and F. Devreux, "On the effect of glass composition in the dissolution of glasses by water," Journal of non-crystalline solids **354**, 117–123 (2008).
[53]C. W. Burnham and N. Davis, "The role of h 2 o in silicate melts; ii, thermodynamic and phase relations in the system naalsi 3 o 8-h 2 o to 10 kilobars, 700 degrees to 1100 degrees c," American Journal of Science **274**, 902–940 (1974).
[54]S. Kohn, R. Dupree, and M. Smith, "A multinuclear magnetic resonance study of the structure of hydrous albite glasses," Geochimica et Cosmochimica Acta **53**, 2925–2935 (1989).
[55]R. Pollet, C. S. Bonnet, P. Retailleau, P. Durand, and É. Tóth, "Proton exchange in a paramagnetic chemical exchange saturation transfer agent from experimental studies and ab initio metadynamics simulation," Inorganic Chemistry **56**, 4317–4323 (2017).
[56]O. Saengsawang, T. Remsungnen, S. Fritzsche, R. Haberlandt, and S. Hannongbua, "Structure and energetics of water- silanol binding on the surface of silicalite-1: Quantum chemical calculations," The Journal of Physical Chemistry B **109**, 5684–5690 (2005).
[57]A. Bankura, V. Carnevale, and M. L. Klein, "Hydration structure of salt solutions from ab initio molecular dynamics," The Journal of Chemical Physics **138**, 014501 (2013).
[58]T. Ikeda, M. Boero, and K. Terakura, "Hydration of alkali ions from first principles molecular dynamics revisited," The Journal of Chemical Physics **126**, 01B611 (2007).
[59]S. S. Azam, T. S. Hofer, B. R. Randolf, and B. M. Rode, "Hydration of sodium (i) and potassium (i) revisited: a comparative qm/mm and qmcf md simulation study of weakly hydrated ions," The Journal of Physical Chemistry A **113**, 1827–1834 (2009).
[60]Y. Zeng, J. Hu, Y. Yuan, X. Zhang, and S. Ju, "Car-parrinello molecular dynamics simulations of na+ solvation in water, methanol and ethanol," Chemical Physics Letters **538**, 60–66 (2012).
[61]C. N. Rowley and B. Roux, "The solvation structure of na+ and k+ in liquid water determined from high level ab initio molecular dynamics simulations," Journal of Chemical Theory and Computation **8**, 3526–3535 (2012).
[62]T. Megyes, S. Bálint, T. Grósz, T. Radnai, I. Bakó, and P. Sipos, "The structure of aqueous sodium hydroxide solutions: A combined solution x-ray diffraction and simulation study," The Journal of Chemical Physics **128**, 044501 (2008).
[63]R. Mancinelli, A. Botti, F. Bruni, M. Ricci, and A. Soper, "Hydration of sodium, potassium, and chloride ions in solution and the concept of structure maker/breaker," The Journal of Physical Chemistry B **111**, 13570–13577 (2007).
[64]M. Galib, M. Baer, L. Skinner, C. Mundy, T. Huthwelker, G. Schenter, C. Benmore, N. Govind, and J. L. Fulton, "Revisiting the hydration structure of aqueous na+," The Journal of Chemical Physics **146**, 084504 (2017).
[65]N. Skipper and G. Neilson, "X-ray and neutron diffraction studies on concentrated aqueous solutions of sodium nitrate and silver nitrate," Journal of Physics: Condensed Matter **1**, 4141 (1989).
[66]J. Mahler and I. Persson, "A study of the hydration of the alkali metal ions in aqueous solution," Inorganic Chemistry **51**, 425–438 (2012).
[67]I. Bako, J. Hutter, and G. Palinkas, "Car–parrinello molecular dynamics simulation of the hydrated calcium ion," The Journal of chemical physics **117**, 9838–9843 (2002).
[68]G. Palinkas and K. Heinzinger, "Hydration shell structure of the calcium ion," Chemical physics letters **126**, 251–254 (1986).
[69]M. Bernal-Uruchurtu and I. Ortega-Blake, "A refined monte carlo study of mg2+ and ca2+ hydration," The Journal of chemical physics **103**, 1588–1598 (1995).

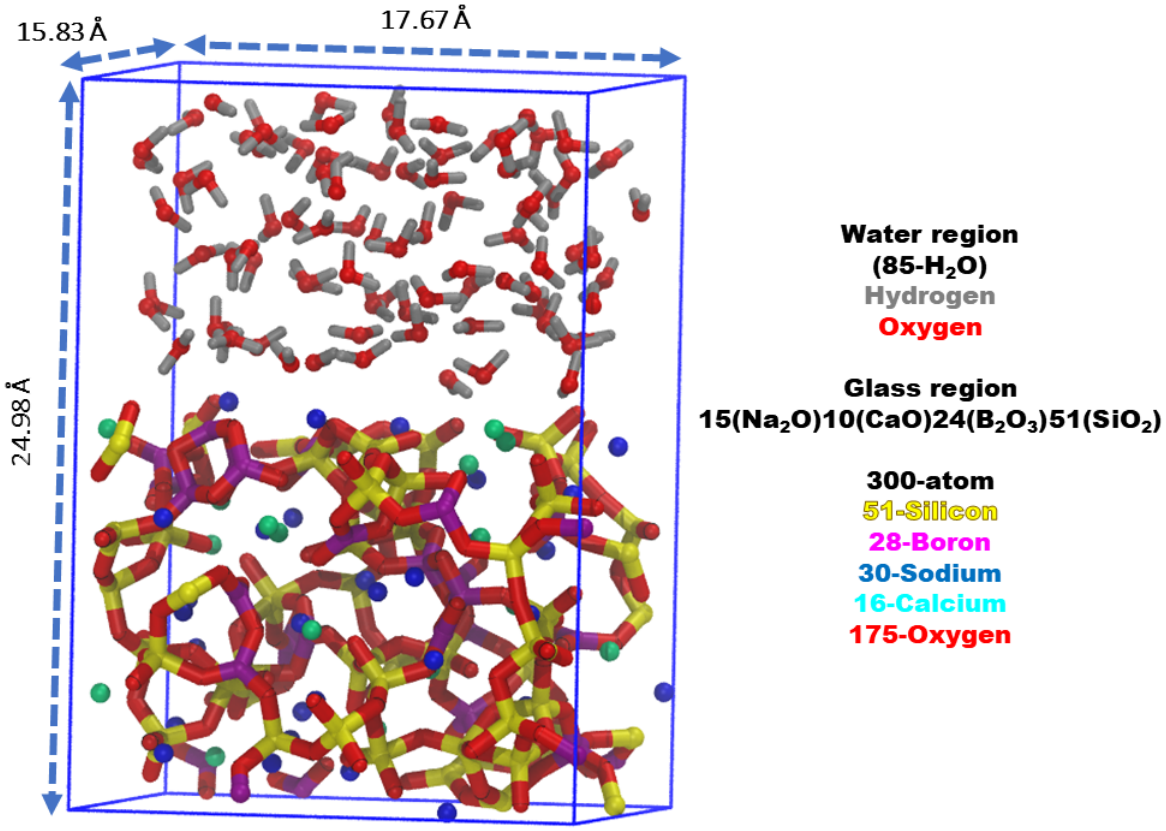

FIG. 1. The structural model of the CNBS glass−water interface before performing CP-AIMD simulations, where a film of 85 water molecules and CNBS glass containing 300 atoms are concatenated.

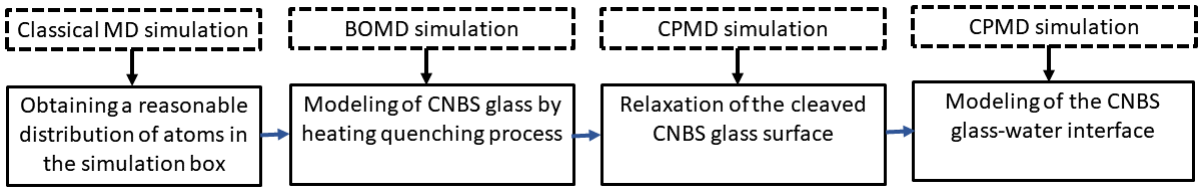

Scheme 1. Simulation methodologies used in our study.

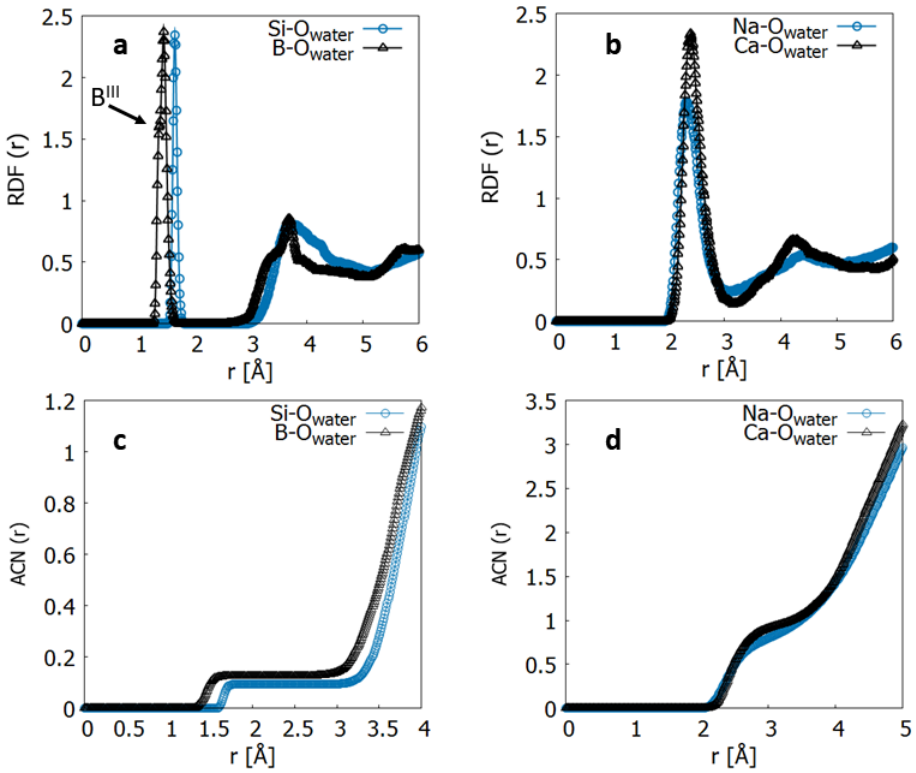

FIG. 2. (a-b) B−O_W, Si−O_W, Na−O_W, and Ca−O_W partial RDFs, (c−d) B−O_W, Si−O_W, Na−O_W, and Ca−O_W average coordination number (ACN). RDFs were obtained over last 50 ps of the NVT simulation at 363 K.

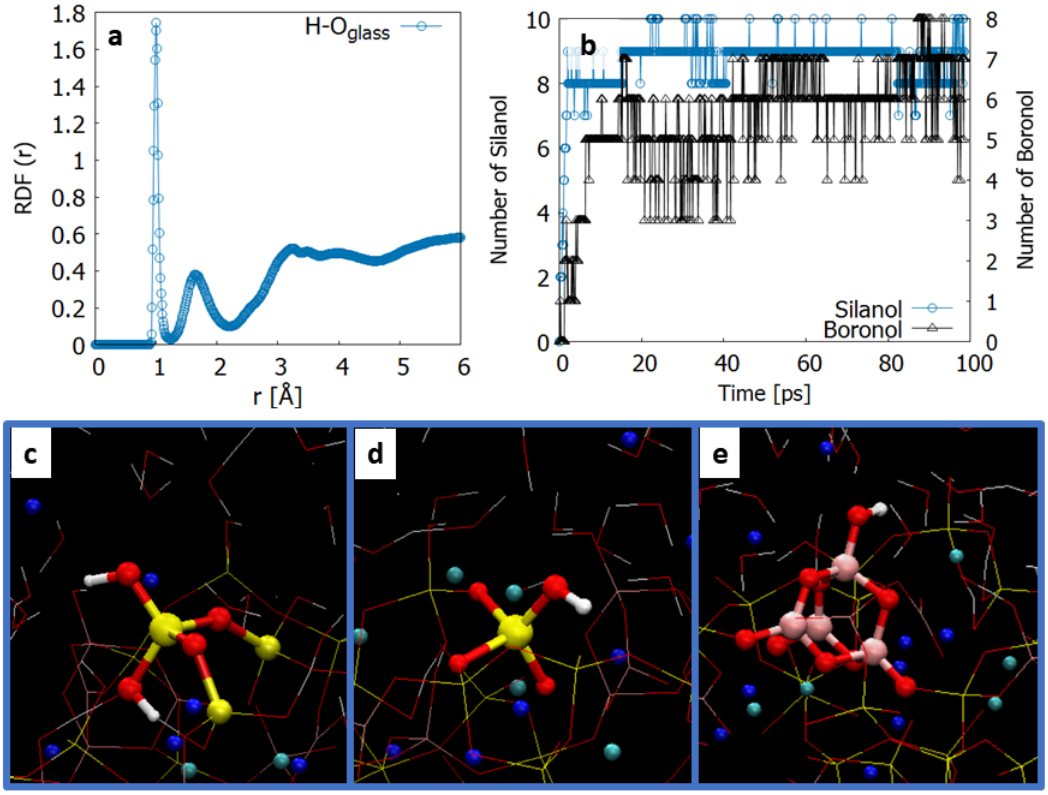

FIG. 3. a) H−O_G RDF of the CNBS glass−water interface, RDF was computed throughout the simulation at 363 K. b) Variation of amount of isolated silanol groups (Si−(OH)) and isolated boronol groups (B−OH) over the whole simulation time, where the functional groups were created after the surface received the proton or hydroxyl group OH from the dissociated water molecules. The snapshots on c), d) and e) represent germinal, silanol and boronol group respectively, where blue, cyan, red, white and yellow balls represent Na, Ca, O, H and Si atoms, respectively. Noteworthy, germinal group is present in insignificant quantity only one group on the whole of the trajectory.

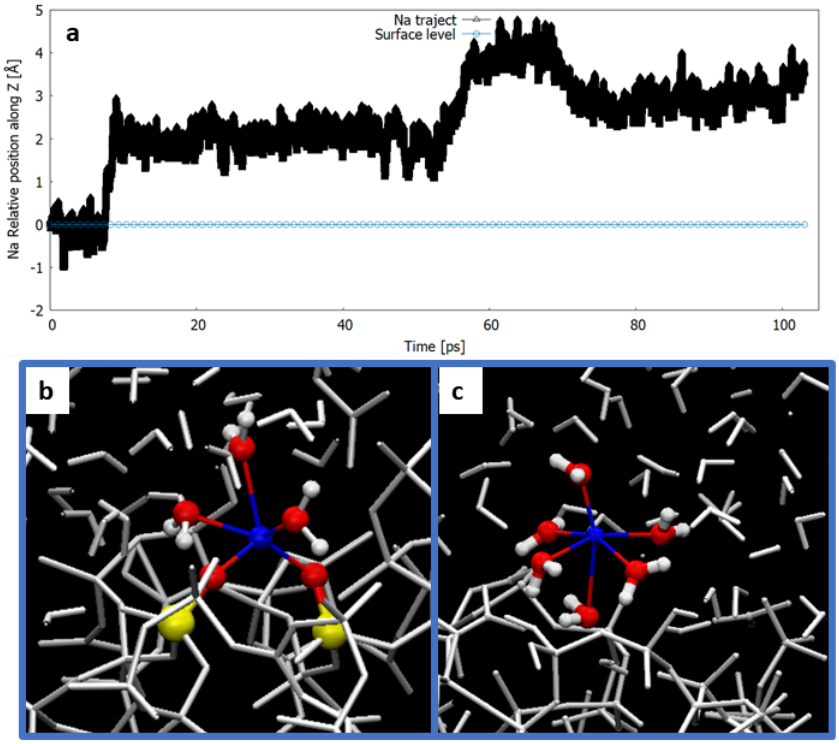

FIG. 4. (a) Monitoring of the relative position of a representative case of the release of Na^+ ions over 100 ps (whole simulation time). (b−c) Snapshots showing the main steps in the trajectory of sodium ion as they diffuse and release from the glass surface to liquid water. Where blue, red, white and yellow balls represent Na, O, H and Si atoms, respectively

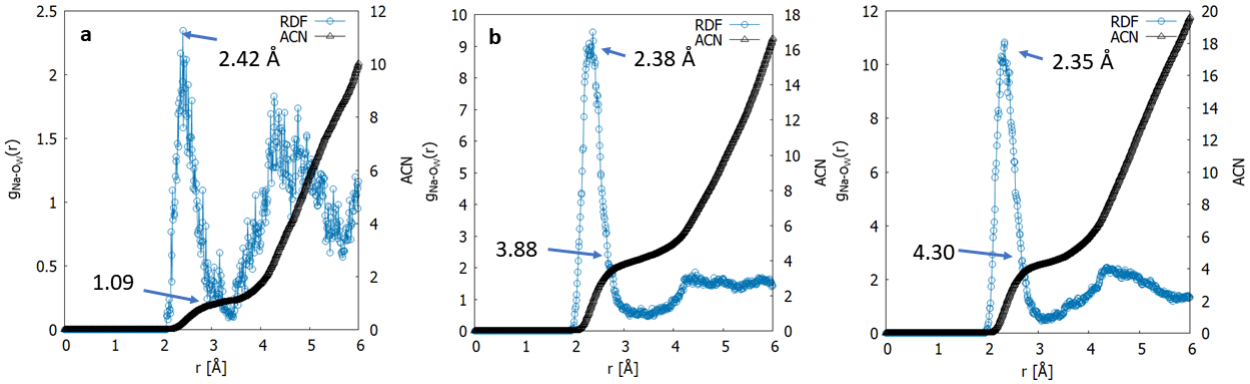

FIG. 5. (a-c) $Na-O_{water}$ RDF and the average coordination number (accumulated RDF function) of the released Na^+ with respect to surrounding water molecules. Where RDF and ACN functions represented on (a) are calculated over the first 5ps, (b) are calculated over a simulation time from 5ps to 55ps, and (c) are calculated over a simulation time from 55ps until the end.

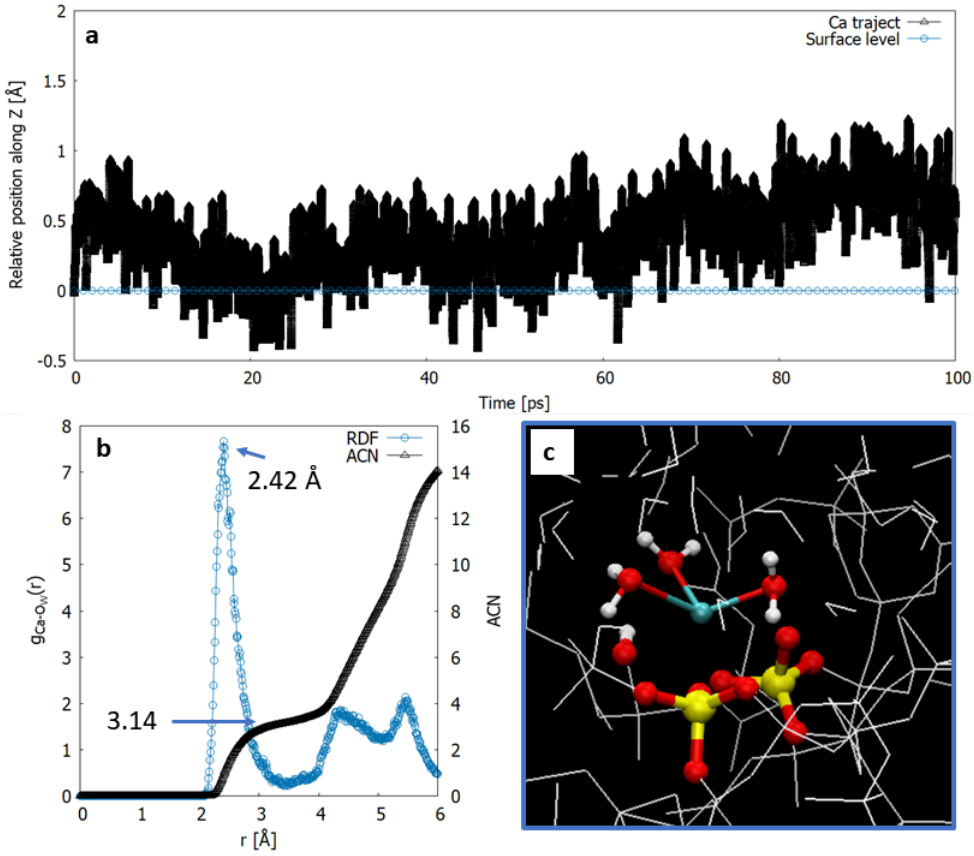

FIG. 6. (a) Monitoring of the relative position of the representative case of the behavior Ca^{2+} ions with water molecules at the interface over whole simulation time. (b) $Ca^{III} - O_W$ RDF and its corresponding average coordination numbers (ACN) with respect to surrounding where RDF and ACN were obtained over the last 50 ps of our trajectory. (c) Snapshot showing how Ca^{2+} ions can interact with water molecules. Where cyan balls represent Ca, red balls represent O, white balls represent H atoms, and yellow balls represent Si.

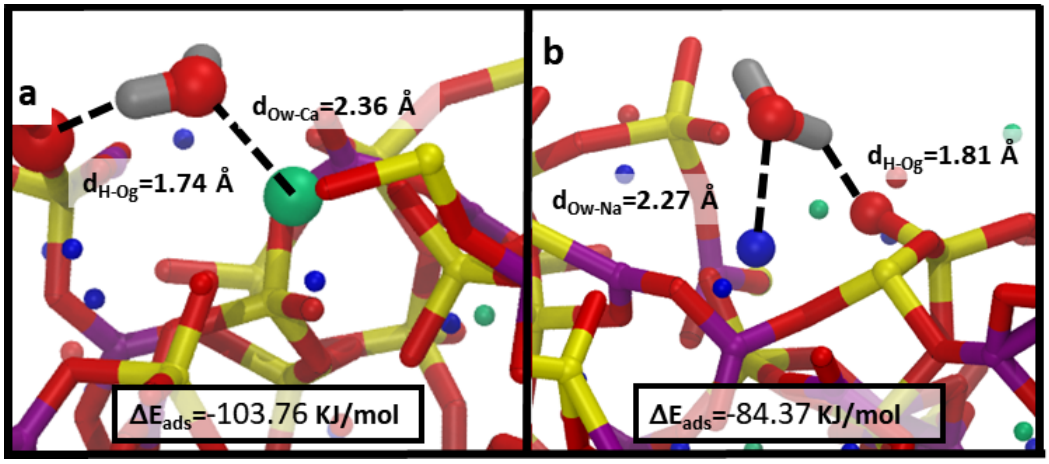

FIG. 7. (a−b) Adsorption of water onto Ca and Na adsorption sites, respectively. Where pink balls represent B, yellow balls represent Si, red balls represent O, blue balls represnts Na, cryan balls represent Ca, and white balls represent H atoms.